

# Angle-resolved $I$ - $V$ characteristics measurements in $\text{Bi}_{1.8}\text{Pb}_{0.2}\text{Sr}_2\text{CaCu}_2\text{O}_{8+\delta}$ single crystals with inclined columnar defects

L. Ammor,\* B. Pignon, N. H. Hong, and A. Ruyter

*Laboratoire d'Electrodynamique des Matériaux Avancés, UMR 6157 CNRS-CEA, Université F. Rabelais, UFR Sciences, Parc de Grandmont, 37200 Tours, France*

(Received 18 April 2003; revised manuscript received 3 March 2004; published 25 June 2004)

Current-voltage ( $I$ - $V$ ) characteristics have been measured over a wide temperature range in a  $\text{Bi}_{1.8}\text{Pb}_{0.2}\text{Sr}_2\text{CaCu}_2\text{O}_{8+\delta}$  single crystal with tilted columnar defects (CDs). This configuration was compared to a crystal irradiated along the  $c$  axis. Above 40 K and in the vortex solid state, angular measurements reveal a pronounced dip in the dissipation when a magnetic field is applied parallel to the CDs. At  $T \leq 40$  K, the measured  $I$ - $V$  characteristics showed that besides the persistence of the directional pinning at low temperatures, there is a shift from the CDs toward the  $c$  axis. Our samples showed, in the high temperature range ( $T \geq 40$  K) and for  $B_\phi/10 < \mathbf{H} < B_\phi$  (where  $B_\phi$  is the matching field) applied parallel to the CDs, a three-dimensional Bose-glass transition with the same critical exponents as  $z' = 5.3 \pm 0.1$  and  $v' = 1.1 \pm 0.1$  which are in very good agreement with numerical simulations. Our findings support the existence of the Bose-glass-to-liquid transition at  $T_{\text{BG}}(\mu_0 H)$  in the case of tilted columnar defects.

DOI: 10.1103/PhysRevB.69.224511

PACS number(s): 74.72.Hs, 74.25.Qt, 74.62.Dh, 74.25.Dw

## I. INTRODUCTION

The state and dynamics of individual vortices in highly anisotropic high layered superconductors such as  $\text{Bi}_2\text{Sr}_2\text{CaCu}_2\text{O}_{8+\delta}$  (BSCCO) containing columnar defects (CDs) have been intensively investigated by many groups. It is well established that the introduction of different configurations of CDs (tilted with respect to the  $c$  axis or splayed-CDs in BSCCO) generates different vortex structures which are strongly field oriented and temperature dependent.<sup>1-3</sup> A common feature exhibited by these irradiated compounds is a significant enhancement of the pinning properties. In the case of columnar defects parallel to the  $c$  axis and to the applied magnetic field, theoretical<sup>4,5</sup> and experimental<sup>6,7</sup> investigations on various high temperature superconductor (HTS) materials have shown that the pinning improvement is due to the enhancement of the magnetic flux pinning strength. Nelson and Vinokur<sup>5</sup> have considered the theory of pinning by CDs based on the analogy between the vortex system and the physics of two-dimensional (2D) bosons for the case where external field  $\mathbf{H}$  is aligned parallel to the CDs or the  $c$  axis of the crystal. At low temperatures and below the matching field  $B_\phi$  ( $B_\phi = \phi_0/d^2$  where  $\phi_0$  is the elementary flux quantum and  $d$  is the mean distance between defects), a Bose-glass phase has been predicted which has a strong localization of vortex lines on the CDs. At higher temperatures the Bose-glass phase melts into an entangled vortex liquid through a second-order transition at  $T_{\text{BG}}(B)$ . The critical behavior of this transition can be described in terms of the scaling theory with two critical exponents  $z'$  and  $v'$ . According to the predictions of Nelson and Vinokur for a Bose-glass transition in the presence of 1D correlated disorder, dynamical predictions for transport measurements with current density  $J$  applied perpendicular to CDs can be expressed as

$$(E/J) = (\xi_{\parallel}/\xi_{\perp}^{z'}) F_{\pm} \left( \frac{J \xi_{\parallel} \xi_{\perp} \phi_0}{K_B T} \right), \quad (1)$$

where  $E(\propto V)$  is the electric field,  $J(\propto I)$  is the current density, and  $F_+$  and  $F_-$  are two scaling functions defined in the flux liquid state ( $T > T_{\text{BG}}$ ) and localized flux-line state ( $T < T_{\text{BG}}$ ), respectively.  $\xi_{\parallel}$  and  $\xi_{\perp}$  measure the corresponding localization lengths of the vortex lines in the directions which are parallel and perpendicular to the columnar defects. In the small current limit, one expects that above  $T_{\text{BG}}$  the scaling function  $F_+(x) \rightarrow \text{constant}$  as  $x \rightarrow 0$ , leading to an ohmic resistivity, as expected for the region above  $T_{\text{BG}}$  in the thermally dominated vortex-liquid. Below  $T_{\text{BG}}$ ,  $F_-(x \rightarrow 0) \approx \exp(x^{-1/3})$  describes the glassy behavior of the system. When approaching the transition,  $F_{\pm}(x) \approx x^{(z'-2)/3}$  as  $x \rightarrow \infty$  with the result that  $\rho \approx J^{(z'-2)/3}$  remains finite at  $T = T_{\text{BG}}$ . At  $T = T_{\text{BG}}$ , the  $E(J)$  curves are expected to show a power law dependence  $E \approx J^{(z'+1)/3}$ . In  $F_{\pm}(x)$ , the current density is expressed as  $J_x = K_B T / (\xi_{\parallel} \xi_{\perp} \phi_0)$  with  $J_x(0) = K_B T / [\phi_0 \xi_{\parallel}(0) \xi_{\perp}(0)]$ . Here,  $J_x(T)$  is defined as a current crossover corresponding to a balance between the thermal energy and the work done by the Lorentz force acting on typical vortex-loop fluctuations of area  $\sim \xi_{\parallel}(t) \xi_{\perp}(t)$ . The anisotropy of pinning properties due to the uniaxial nature of the defects leads to  $\xi_{\perp}(T) = \xi_{\perp}(0) |(T - T_{\text{BG}})/T_{\text{BG}}|^{-\nu_{\perp}}$  and  $\xi_{\parallel}(T) = \xi_{\parallel}(0) |(T - T_{\text{BG}})/T_{\text{BG}}|^{-\nu_{\parallel}}$ , where  $\nu_{\parallel} \equiv 2\nu_{\perp} \equiv 2v'$  in the case of anisotropic correlation volume.  $z'$  and  $v'$  denote the critical exponents governing the thermal relaxation time  $\tau[\tau(T) \approx \xi_{\perp}^{z'}(T)]$  and transverse correlation length of fluctuations of the flux lines, respectively.

In  $\text{YBa}_2\text{Cu}_3\text{O}_{7-\delta}$  single crystals and films containing CDs along the  $c$  axis, the existence of a Bose-glass transition has been confirmed by the critical behavior of the ac and dc

conductivities at  $T_{BG}$ .<sup>8–10</sup> In BSCCO, a second order Bose-glass transition was demonstrated by transport measurements<sup>11</sup> and by numerical simulations<sup>12</sup> through the critical scaling of current-voltage characteristics. When  $\mathbf{H}$  is tilted at angle  $\psi$  away from the column direction, the Bose-glass phase with perfect alignment of the internal flux density  $\mathbf{B}$  parallel to the columns is predicted to be stable up the critical transverse field  $\mathbf{H}_{\perp c}$  producing the so-called Meissner effect (TME). More recently, the TME has been observed by transport measurements in BSCCO when the applied field is tilted up to an angle of  $\psi_c \approx 20^\circ$  away from the column direction which is smaller than the lock-in angle.<sup>13</sup> The fact that the Bose-glass behavior is typically observed above 40 K clearly indicates a line nature of the vortices, in contrast to low temperature experiments which shows isotropic pinning in this material.<sup>14,15</sup>

Previous experiments on vortex pinning properties by columnar defects tilted with respect to the crystallographic  $c$  axis have also been carried out on BSCCO single crystals.<sup>16–18</sup> Tilted CDs have been used to distinguish their pinning from intrinsic anisotropy effects. Generally, most of the reported results on tilted CDs indicate two distinct temperature regimes.<sup>2,14,15,17</sup> At high temperatures ( $T > 40$  K), the angular magnetic and transport measurements confirm the maximum pinning when the magnetic field is aligned with the inclined CDs. However, so far, an experimental evidence of the presence of a Bose-glass transition in this configuration, which might be manifested by universal scaling behavior, has not been shown. At low temperatures ( $T \leq 40$  K), the pinning is isotropic. In this regime, the magnetization curves measured with applied field at various directions relative to the CDs are almost indistinguishable.<sup>2</sup> The crossover between these two regimes seems to shift to a lower temperature as the anisotropy decreases. Note that other groups attributed the absence of unidirectional pinning in the low temperature to the 2D nature of BSCCO.<sup>15</sup>

In order to study the effect of tilted tracks on vortex pinning, we have investigated the vortex dynamics over a wide range of temperatures and applied magnetic fields in  $\text{Bi}_{1.8}\text{Pb}_{0.2}\text{Sr}_2\text{CaCu}_2\text{O}_{8+\delta}$  single crystals with tilted and non-tilted CDs by measurements of the  $I$ - $V$  characteristics. It is well known that the pinning properties of BSCCO are very sensitive to the doping level, which can be modified by Pb substitution on Bi sites.<sup>19,20</sup> Thus the Pb doping of BSCCO increases the carrier concentration, which can lead to the overdoped region in the phase diagram in comparison with the Pb-free samples.<sup>21</sup> The heavily Pb-substituted BSCCO shows remarkable increases in the irreversibility line and critical current densities.<sup>22,23</sup> The improved flux pinning properties in heavily Pb doped BSCCO, below a certain threshold of the Pb content, are suggested to originate from the lowered electronic anisotropy, and the existence of strong 3D correlations in the flux line structure due to the Pb doping.<sup>24,25</sup>

The main aim of this work is to compare the pinning properties of a single crystal irradiated at  $\theta_{\text{irr}}=45^\circ$  (where  $\theta_{\text{irr}}$  is the angle between crystallographic axis and the irradiation direction) and another irradiated at  $\theta_{\text{irr}}=0^\circ$  (both with the same density of tracks in the  $ab$  plane). We will report about pinning enhancement in the symmetric orientation  $\psi=-45^\circ$

( $\psi$  is defined as the angle between the applied magnetic field  $\mathbf{H}$  and the crystal  $c$  axis) for crystal containing inclined defects. On the other hand, the static and dynamic critical exponents,  $\nu'$  and  $z'$ , associated with the Bose-glass scaling theory will be determined from the voltage-current behavior.

The remainder of this paper is organized as follows. The sample preparation and experiments are presented in Sec. II. The uniaxial enhancement of pinning for the sample with inclined CDs observed by angular measurements over a large temperature range is presented in Secs. III A ( $T \geq 40$  K) and III B ( $T=20$  K). In Sec. III C we will show that for  $B_\phi/10 < H < B_\phi$  and  $T \geq 40$  K, the same scaling functions can be used to describe the transition in both  $\text{Bi}_{1.8}\text{Pb}_{0.2}\text{Sr}_2\text{CaCu}_2\text{O}_{8+\delta}$  single crystals with parallel and tilted columnar defects, which emphasizes the universality of this transition. Finally, the temperature-field phase diagram derived from scaling analysis is discussed on the basis of the theory of Nelson and Vinokur and compared with those obtained previously on BSCCO single crystals<sup>11</sup> (Sec. III D).

## II. EXPERIMENT

Experiments were performed on two  $\text{Bi}_{1.8}\text{Pb}_{0.2}\text{Sr}_2\text{Ca}_1\text{Cu}_2\text{O}_{8+\delta}$  single crystals. Both samples were grown by a self-flux method which has been described elsewhere.<sup>21</sup> The samples with typical dimensions of  $0.4 \times 1 \times 0.02$  mm<sup>3</sup> were irradiated at Ganil (Caen, France) with a beam of 6 GeV Pb ions (which traversed over the entire specimen). As for sample A, parallel CDs of diameter  $\approx 90$  Å were created for one crystal along the  $c$  axis and for sample B the beam was oriented at an angle of  $45^\circ$  with respect to the  $c$  axis.<sup>26</sup> Fluences of  $\phi_t=3.75 \times 10^{10}$  cm<sup>-2</sup> (i.e.,  $B_\phi=0.75$  T), and  $\phi_t=5.25 \times 10^{10}$  cm<sup>-2</sup> (i.e.,  $B_\phi \approx 1$  T) were chosen to irradiate samples A and B, respectively. Such a fluence  $B_\phi \approx 1$  T, for sample B, has been chosen in order to obtain a planar density of tracks  $n_{\text{CD}}$  in the  $(a,b)$  planes [ $n_{\text{CD}}=\phi_t \cos(45^\circ)$ ] corresponding to a matching field of 0.75 T. Isothermal  $I$ - $V$  characteristics were obtained by using a standard dc four-probe method with a voltage resolution of 0.5 nV and a temperature stability better than 5 mK. Sample A has a superconducting transition temperature  $T_{c0}$  (determined by using the inflection point of the resistive transition) of 78.4 K, while sample B has a  $T_{c0}$  of 78 K. After irradiation,  $T_{c0}$  of samples A and B was found to decrease by  $\sim 5$  K compared to the unirradiated reference sample. The transition width  $\Delta T_{c0}$  was approximately  $\Delta T_{c0}=1.0$ – $1.5$  K. The anisotropy parameter,  $\gamma \sim 60$ , was estimated by resistivity measurements on the unirradiated reference sample using the same procedure as Ref. 27. For comparison, similar results for Pb-substituted BSCCO single crystals with nominal compositions  $\text{Bi}_{1.6}\text{Pb}_{0.4}\text{Sr}_2\text{CaCu}_2\text{O}_{8+\delta}$  ( $\gamma \approx 68$ )<sup>28</sup> and  $\text{Bi}_{1.8}\text{Pb}_{0.4}\text{Sr}_2\text{CaCu}_2\text{O}_y$  ( $\gamma \approx 100$ )<sup>22</sup> were reported. The angular dependence of the voltage measurements was systematically investigated on Pb-substituted BSCCO single crystals before irradiation. The  $V(\psi)$  does not exhibit a dip at any direction of the applied field, while in the case of samples irradiated along the  $c$  axis the dip is a typical feature of the anisotropic pinning induced by CDs.

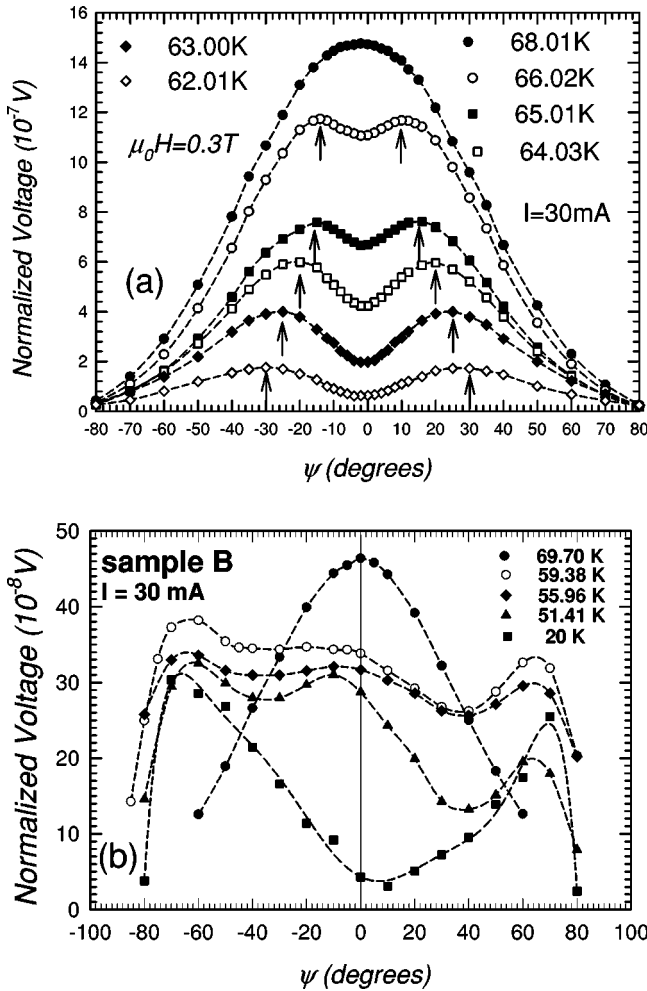


FIG. 1.  $V(\psi)$  curves measured in solid state with  $I=30$  mA at various temperatures for (a) sample A and (b) sample B after irradiation.

### III. RESULTS AND DISCUSSIONS

#### A. Angular dependence of the voltage

The angular dependence of the voltage measurements  $V(\psi)$  at a fixed current was systematically investigated for samples A and B. Typical  $V(\psi)$  curves for  $\mu_0 H = 0.3$  T taken at several temperatures above and below the Bose-glass melting temperature are shown in Fig. 1(a) for the sample containing CDs parallel to the  $c$  axis and in Fig. 1(b) for the sample containing tilted columnar defects. For the lowest  $T$  and  $H < B_\phi$  values, the  $V(\psi)$  curves exhibit a pronounced dip at  $\psi = 0$  (sample A) and  $\psi = 45^\circ$  (sample B) in the vortex solid state when the magnetic field is applied parallel to the CDs. This pronounced downward dip of dissipation around  $\mu_0 H \parallel$  CDs is ascribed to CDs pinning. When the magnetic field is tilted away from the direction of the CDs, the dissipation increases with increasing angle, indicating that the pinning by CDs remains effective up to the accommodation angle  $\psi_a$  [the accommodation angle  $\psi_a$  is determined experimentally as half the angular width between voltage maxima indicated by arrows in Fig. 1(a)]. The accommodation angle is about  $\psi_a \approx 30^\circ$  and  $25^\circ$  at  $T = 62.01$  and  $51.41$  K for samples A and

B, respectively. This increase of the voltage has been related to vortex pinning by CDs, with  $\psi_a$  the limit of the effectiveness of CDs pinning. Above  $\psi_a$ , the pinning by CDs disappears and the dissipation is more controlled by the intrinsic pinning. These results clearly confirm a strong localization of the vortex on the columnar defects when they are aligned. Such a strong angular dependence of pinning is expected for 3D vortices, but not for the extremely weak coupling 2D pancake vortices. Similar features have been previously observed by transport measurements on both moderately anisotropic layered cuprates such as  $\text{Bi}_2\text{Sr}_2\text{CuO}_y$  (Bi-2201) thin films<sup>29</sup> and on highly anisotropic material such as  $\text{Bi}_2\text{Sr}_2\text{CaCu}_2\text{O}_{8+\delta}$  (Refs. 7 and 30) and  $\text{Tl}_2\text{Ba}_2\text{CaCu}_2\text{O}_8$ .<sup>6,31</sup> In contrast, for extremely anisotropic  $\text{Bi}_2\text{Sr}_2\text{CaCu}_2\text{O}_8/\text{BiSr}_2\text{CuO}_6$  multilayers<sup>32</sup> and  $\text{YBa}_2\text{Cu}_3\text{O}_{7-\delta}/\text{PrBa}_2\text{Cu}_3\text{O}_{7-\delta}$  superlattices,<sup>33</sup> there has been no directional effect at all. This result has been explained by a strong 2D behavior of these latter materials. Figure 1(b) clearly shows that tilted defects also improve the pinning efficiency for magnetic fields applied parallel to the CDs. These results contrast with magnetization and transport measurements at high temperatures in BSCCO single crystals and BSCCO thin films irradiated under various irradiation angles with respect to the  $c$  axis where an enhanced pinning by the CDs was found to be isotropic.<sup>34,35</sup> The dependence of the critical current density (determined from magnetization measurements) on the magnetic field and its orientation consistently indicates two-dimensional pinning of pancake vortices at the CDs. In these two reports, no irradiation induced directional pinning can be observed when the external magnetic field is continuously rotated with respect to CDs. Furthermore, it has been shown that the pinning enhancement by tilted columnar defects from the  $c$  axis can be related to an increase of pinning energy resulting from the enlargement of the defects cross section in the  $\text{CuO}_2$  planes.<sup>36-38</sup>

Another major feature observed for sample B is an anomalous minimum centered along the direction perpendicular to the columnar defects. This is the first time, to the best of our knowledge, that a less pronounced dip at  $\psi = -45^\circ$  (in addition to the one at  $\psi = +45^\circ$ ) has been observed by transport measurements. The enhancement of this pinning efficiency for  $\psi = -45^\circ$  might be related to a flux flop phenomenon. This behavior has already been observed by magnetic measurement on  $\text{Bi}_2\text{Sr}_2\text{CaCu}_2\text{O}_8$  single crystals irradiated at  $45^\circ$  from the  $c$  direction.<sup>15,17</sup> Similar to what is observed in a lock-in transition towards the  $\text{CuO}_2$  planes in layered HTSCs,<sup>4</sup> the vortex in the configuration of the applied field perpendicular ( $\psi = -45^\circ$ ) to the CDs flop toward the direction of defects below a critical field of  $\mu_0 H_c \approx 0.001$  T at 50 K.<sup>2</sup> While the  $\mu_0 H \approx 0.3$  T in our experiment is much larger than that, it approaches the experimental value as  $\mu_0 H \approx 0.1$  T reported by Kazumata *et al.*<sup>17</sup> Moreover, recent experiments using Lorentz microscopy at temperature above  $T = 19$  K on BSCCO films irradiated at  $70^\circ$  indicated that vortex lines remain trapped along defects even when a magnetic field was applied in the direction of  $\psi = -70^\circ$ .<sup>39</sup>

#### B. Low-temperature vortex dynamics

$I(V)$  curves as a function of the angle  $\psi$  (between the applied field and the  $c$  axis), which were taken at 20 K under

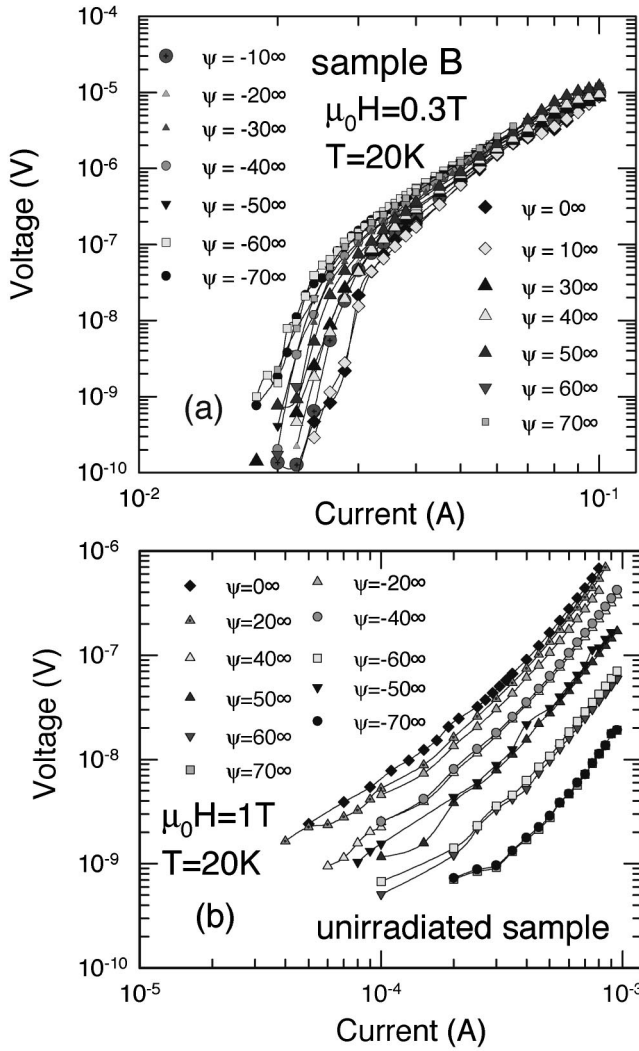


FIG. 2. The angular dependence of the isothermal  $I$ - $V$  curves measured at  $T=20$  K for (a) sample containing inclined columnar defects at a field of 0.3 T and (b) as-grown Pb-substituted BSCCO crystal in applied field  $\mu_0 H=0.3$  T.

a magnetic field of 0.3 T, are shown in Fig. 2(a). The typical  $I$ - $V$  curves measured at 20 K before irradiation in a magnetic field of  $\mu_0 H=1$  T is demonstrated in Fig. 2(b) in order to compare. As seen from Fig. 2(a), the isothermal curves clearly show a downward curvature in the angular range from  $-70^\circ$  to  $+70^\circ$  which is typical for the glassy vortex system at low temperatures. This result is quite different from what was observed in the unirradiated reference sample [see Fig. 2(b), where a positive curvature is usually analyzed in terms of the flux-creep approach<sup>40</sup>]. The glassy behavior observed at low temperatures in the sample containing tilted defects reflects the pinning by CDs for all orientations of the applied field investigated. One can notice that there is no more measurable creep phenomena at low current due to the low temperature. In fact, the vortex velocity is more strongly temperature dependent than even the activation energy itself. Thus measurements are decreased by almost a factor almost equal to  $\exp(-\alpha)$  when the temperature is decreased down to low temperature as  $T/\alpha$ . Consequently, the vortex motion

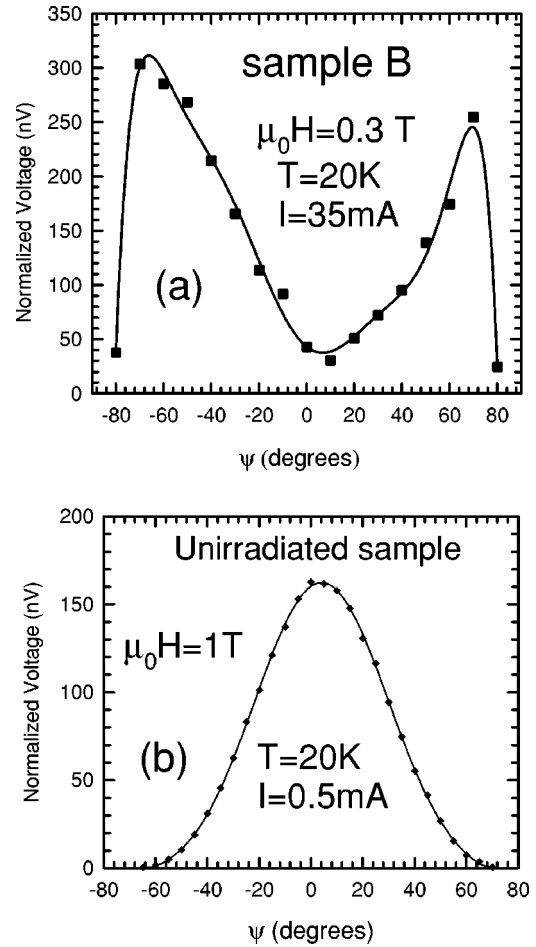


FIG. 3. Typical  $V(\psi)$  measured at 20 K and for a fixed current and the applied magnetic field  $\mu_0 H=0.3$  and 1 T, respectively, (a) the crystal with tilted columnar defects sample B and (b) unirradiated sample.

cannot be described anymore using the functional form:  $V = R_0 I \exp[-U/\beta(I_0/I)^\mu]$  with  $\beta=K_B T$  and  $\mu$  ranging from 1/3 to 1 as predicted for the relevant excitations of the Bose-glass phase (variable range hopping or half loop).<sup>4,5</sup> Moreover, the sudden increase of the velocity suggests a collective depinning mechanism when the applied magnetic field is weak enough. Furthermore, it appears that the dip at CDs angular position which was observed before, shifts away from the CDs towards the  $c$  axis [see Fig. 1(b)]. Figure 3 shows typical  $V(\psi)$  curves measured at 20 K using a fixed current and an applied magnetic field for the crystal with tilted CDs ( $\mu_0 H=0.3$  T) and the unirradiated sample ( $\mu_0 H=1$  T), respectively. The most prominent feature of this figure is a strongly anisotropic pinning observed when  $H \parallel c$  axis (i.e., mid-direction between the defect and  $\psi=-45^\circ$  directions) rather than along the direction of the defects at  $\psi=45^\circ$ . A comparable behavior was reported by Silhanek *et al.*<sup>41</sup> for  $\text{YBa}_2\text{Cu}_3\text{O}_{7-\delta}$  and  $\text{ErBa}_2\text{Cu}_3\text{O}_{7-\delta}$  single crystals with inclined columnar defects. In this study, the shift away from the CDs towards the  $c$  axis was observed by the angular dependence of the irreversible magnetization measurements for  $\mu_0 H < 1$  T and  $T \geq 60$  K. It was shown that the shift results from the misalignment between vortices and the applied

field direction in anisotropic materials. The combined pinning by the simultaneous presence of twin boundaries, tilted CDs, and crystallographic  $ab$  planes, which generates a variety of complex staircases, likely explains the angular shift in this compound. This scenario could be an explanation of our observations if we replace the twin boundaries by the laminar microstructures (LMs) parallel to the  $a$  axis observed with transmission electron microscopy measurement of the  $\text{Bi}_{2-y}\text{Pb}_y\text{Sr}_2\text{CaCu}_2\text{O}_{8+\delta}$  single crystals in the case of  $y=0.6$ .<sup>23,42</sup> In  $y=0.6$  samples, the LMs act as planar pinning centers for a wide range of the applied field orientation ( $\psi \sim 70^\circ$ ).<sup>22,28</sup> However, the recent transmission electron microscopy investigations on  $\text{Bi}_{2-y}\text{Pb}_y\text{Sr}_2\text{CaCu}_2\text{O}_{8+\delta}$  single crystals with different compositions have pointed out that the LMs appears beyond a certain threshold in the Pb content  $y=0.4$ .<sup>43,44</sup> This value is higher than that of our moderately Pb-doped crystals ( $y=0.2$ ). This result is in favor of the data obtained by the angular measurements performed in both solid and liquid phases of our  $\text{Bi}_{1.8}\text{Pb}_{0.2}\text{Sr}_2\text{CaCu}_2\text{O}_{8+\delta}$  samples, which do not show any additional defects effect before irradiation.

Other studies have addressed the similar improvements of the pinning efficiency around the  $c$  axis. In general, they were obtained at higher temperatures ( $T \geq 60$  K) in  $\text{YBa}_2\text{Cu}_3\text{O}_{7-\delta}$  single crystals<sup>45</sup> and thin films<sup>46</sup> containing splayed columnar defects or two sets of tilted defects in Bi-2212 single crystal<sup>16</sup> and in  $\text{YBa}_2\text{Cu}_3\text{O}_{7-\delta}$  thin films.<sup>47</sup> In all of these cases, angular transport and magnetic measurements indicated that a maximum of the critical current density  $J_c$  and of the irreversibility temperature  $T_{\text{irr}}$  are obtained when the magnetic field is applied along the  $c$  axis. This strong pinning is related to the fact that, for this symmetry direction ( $\mathbf{H} \parallel c$ ), a kinked vortex structure (staircases) between differently oriented tracks should be favored. Another parameter, which plays an important role in determining the vortex elastic and the pinning energies, is the anisotropy  $\gamma$ . In the highly anisotropic BSCCO, the larger  $\gamma$  in this system influences the pinning due to the CDs more than the weakly anisotropic  $\text{YBa}_2\text{Cu}_3\text{O}_7$ . The combined effect of correlated and intrinsic pinning, depending on the temperature and the field orientation, produces a variety of complex staircases. Our results show that the kinked structures dominate the vortex pinning at low temperature.

In conclusion, the dip shift which was observed at low temperature from inclined tracks direction to the  $c$  axis with decreasing  $T$ , could be associated to a partially pinned staircases vortex structure. The origin and detailed physical nature of the pronounced dip for  $\psi = -45^\circ$  and the dip shift observed with decreasing temperature remain as open questions.

### C. Scaling analysis of current-voltage characteristics

Figures 4(a) and 4(b) show the angle dependence of the voltage for samples A and B while the applied magnetic field  $\mathbf{H}$  was aligned with the tracks using the well-known dip feature occurring in the dissipation process for  $\psi_{\text{min}} \approx -0.6^\circ$  and  $44.3^\circ$ .

We examined the shape of the  $I$ - $V$  curves in the vicinity of the glass-liquid transition at well-defined temperatures from

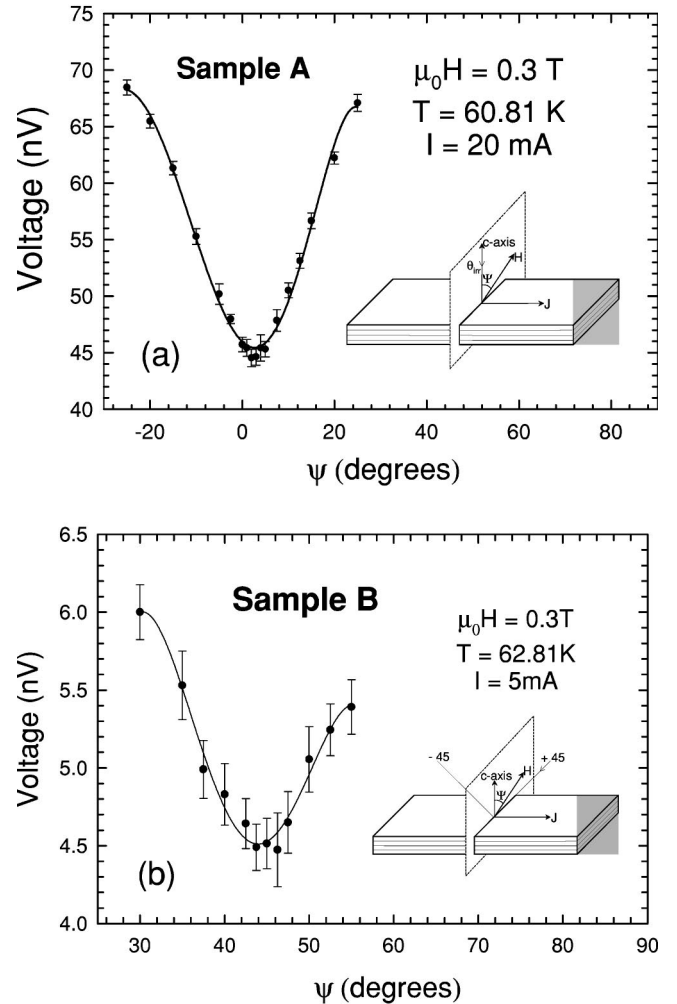


FIG. 4. Typical angular dependence of the voltage at a fixed current. The angle  $\psi$  is measured between the  $c$  axis and the applied magnetic field for (a) sample A and (b) sample B. The applied magnetic field  $\mathbf{H}$  was aligned with the CDs using the well-known dip feature occurring in the dissipation at  $\psi_{\text{min}} \approx -0.6^\circ$  and  $\approx -44.3^\circ$  for samples A and B, respectively. The schematic representation of the irradiation and measurements directions is also shown. The irradiation directions correspond to  $\theta_{\text{irr}}=0$  for parallel and  $\theta_{\text{irr}}=45^\circ$  for inclined columnar defects with respect to the  $c$  axis.

a resistive state into a superconducting state ( $R \equiv V/I=0$ , in the low current density limit) upon cooling, in an applied magnetic field lower than  $B_\phi$  along the CDs direction and above 40 K. For a fixed filling fraction  $f$  (i.e.,  $f \equiv \mu_0 H / B_\phi$ ) which is smaller than 1, the typical isothermal  $I$ - $V$  curves measured for samples A and B reveal a negative curvature in the low temperature region as expected for a glassy vortex system.<sup>11</sup> Such typical behavior can be explained on the basis of the Bose-glass melting theory.<sup>4,5</sup>

In general, the estimated values of the dynamic exponent  $z$  and the static exponent  $\nu_\perp$  are derived from a power law dependence  $V \sim I^{(z+1)/(1+\alpha)}$  at  $T=T_{\text{BG}}$  and the fitting of the ohmic resistance (linear part of  $I$ - $V$  curves in the limit  $I \rightarrow 0$ ) near  $T_{\text{BG}}$  in the thermally assisted flux-flow regime which should vanish according to  $R \sim [(T$

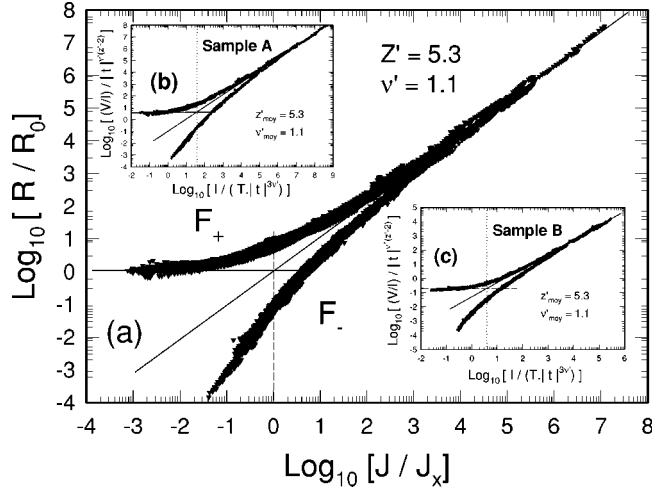


FIG. 5. Bose-glass scaling of the  $I$ - $V$  characteristics at different temperatures and in different applied magnetic fields parallel to CDs. (a) Universal scaling forms for the resistance were obtained in both samples over a wide range of filling factors  $0.026 \leq f \leq 0.9$ . The scaling obtained in (b) and (c) was normalized by  $R_0$  and  $I_x$ .  $I_x$  is the current crossover separating the ohmic regime from the non-ohmic regime. The same scaling exponents  $z' = 5.3 \pm 0.1$  and  $v' = 1.10 \pm 0.1$  are used for all fields. According to Eq. (1), the upper and lower branches display Bose-glass universal functions  $F_+$  and  $F_-$  above and below the critical temperature  $T_{BG}$ , respectively. Insets are scaling forms for the resistance above and below  $T_{BG}$  at different filling factors of  $0.023 \leq f \leq 0.9$  for samples A and B, respectively. (b) is for sample A with  $f = 0.1, 0.133, 0.267, 0.4, 0.67, 0.8,$  and  $0.9$ . (c) is for sample B with  $f = 0.075, 0.1, 0.2, 0.3, 0.4, 0.5, 0.75,$  and  $0.9$ . The solid lines represent asymptotic behaviors, and their crossing identifies the quantity  $I_x(0)$  for  $T > T_{BG}$ .

$-T_{BG}/T_{BG}]^{v_{\perp}(z-2)}$ . Since  $R$  follows the above power law, a plot of  $(d \ln R/dT)^{-1} = (T - T_{BG})/[v_{\perp}(z-2)]$  versus temperature should be a straight line with a slope equal to  $1/[v_{\perp}(z-2)]$  intercepting the temperature axis at  $T_{BG}$ . The plot of  $(d \ln R/dT)^{-1} = (T - T_{BG})/[v_{\perp}(z-2)]$  versus temperature is consistent with this type of behavior. Combining these two measurements, we obtained  $v_{\perp} \sim 1$  and  $z \sim 5$ . Our experimental observations do not show any signature of the vortex molasses scenario (VM) as reported by Reichhard *et al.*<sup>48</sup> In the VM scenario, one expects the resistivity to follow the Vogel-Fulcher law as  $\rho(T) = \rho_{VM} \exp[-1/(T - T_G)]$ , whereas in the Bose-glass theory the resistivity vanishes as  $\rho(T) \sim [(T - T_{BG})/T_{BG}]^{v_{\perp}(z-2)}$ .

Figure 5 shows the best scaling collapses of the whole set of  $I$ - $V$  characteristics which are consistent with Eq. (1) for both samples using  $z' = 5.3 \pm 0.1$  and  $v' = 1.1 \pm 0.1$ . The same critical exponents were obtained for both samples over a wide range of filling fractions of  $0.133 \leq f \leq 0.8$ . Two experimental observations are presented in Figs. 5(b) and 5(c). First, the  $I$ - $V$  data nicely collapse into the upper (ohmic:  $T > T_{BG}$ ) and lower (non-ohmic:  $T < T_{BG}$ ) scaling branches. From asymptotic behaviors of scaling functions  $F_+$  (upper branch  $T > T_{BG}$ ) and  $F_-$  (lower branch  $T < T_{BG}$ ), we have extracted two quantities  $R_0$  and  $I_x(0)$ , which can be related to the sample's normal resistance and vortex-loop area, respectively. As shown in Fig. 5, the horizontal and oblique solid

lines show  $F_+(x) = 1$  and  $F_-(x) = x^{(z'-2)/3}$ , respectively. Their intersection point gives  $J_x(0)$  which can be used to evaluate the correlation length. We estimate  $[\xi_{\parallel}(0)\xi_{\perp}(0)]^{1/2} \approx 20\text{--}30 \text{ \AA}$  which is considered to be a physical value and comparable to what was determined in BSCCO single crystals irradiated in the direction which is parallel to the  $c$  axis.<sup>11</sup> Moreover, Figs. 5(b) and 5(c) show that  $R = R_0 t^{v'(z'-2)}$  as  $T \rightarrow T_{BG}^+$  is independent of  $T$  and  $\mathbf{H}$  for both samples. Note that the values of the critical exponents  $z' = 5.3 \pm 0.1$  and  $v' = 1.1 \pm 0.1$  [i.e.,  $v'(z'-2) = 3.63$ ] are found for either sample to be insensitive to  $\mathbf{H}$  over a range of fields corresponding to a filling fraction  $0.133 < f < 0.8$ .

This result is reasonably consistent with numerical studies for the case of strongly screened vortex interactions, which predicted that  $z' = 4.6 \pm 0.3$  and  $v' = 1.00 \pm 0.01$ .<sup>49</sup> It is also in accord with other experimental results where for  $\text{Bi}_2\text{Sr}_2\text{CaCu}_2\text{O}_{8+\delta}$  single crystals with  $v'(z'-2)$  are equal to about 4 (Ref. 50) and for  $\text{Tl}_2\text{Ba}_2\text{CaCu}_2\text{O}_8$  thin films  $z' = 4.9 \pm 0.2$  and  $v' = 1.1 \pm 0.2$  (Ref. 51) or  $z' = 4.4 \pm 0.3$  and  $v' = 1.8 \pm 0.1$ .<sup>6</sup> More recently, Soret *et al.* obtained  $z' = 5.28 \pm 0.05$  and  $v' = 1.04 \pm 0.06$  in irradiated  $\text{Bi}_2\text{Sr}_2\text{CaCu}_2\text{O}_{8+\delta}$  and  $\text{Bi}_2\text{Sr}_2\text{Ca}_{1-x}\text{Y}_x\text{Cu}_2\text{O}_{8+\delta}$  single crystals.<sup>11</sup>

So far, as for tilted CDs, the only reported values for the critical exponents are obtained from the Bose-glass scaling of current-voltage characteristics in  $\text{YBa}_2\text{Cu}_3\text{O}_{7-\delta}$  melt-textured and thin film samples irradiated in splayed configuration of  $\theta_{\text{irr}} = \pm 45^\circ$  and  $\pm 10^\circ$ .<sup>46,52</sup> In the former case, the values  $z' = 4.0 \pm 0.2$  and  $v' = 0.95 \pm 0.2$  are found when the magnetic field is aligned along the columnar defect. In the latter case,  $z' \approx 7.20$  and  $v' \approx 1.25$  are extracted from the critical scaling of  $V(I)$  curves when the magnetic field is applied parallel to the  $c$  axis. We note that field and sample independent values of the critical exponents  $z' = 5.3 \pm 0.1$  and  $v' = 1.1 \pm 0.1$  are consistent with hypothetical universal critical behavior at standard continuous transitions.

The Bose-glass theory gives two distinct predictions: for the dynamics scaling of vortex transport properties and the response to tilted magnetic fields. Such a behavior has been observed in our doped and undoped BSCCO single crystals irradiated parallel to the  $c$  axis.<sup>11,13</sup> The fact that we observe the scaling behavior in Pb-substituted BSCCO single crystals with tilted CDs with the same critical exponents as those observed in doped and undoped BSCCO containing parallel CDs support the Bose-glass picture. This result shows that the vortex dynamics is not sensitive to the doping level, doses, and inclination of irradiation also seem to favor the presence of the Bose-glass transition. The existence of the Bose-glass-to-liquid transition in  $\text{Bi}_{1.8}\text{Pb}_{0.2}\text{Sr}_2\text{CaCuO}_{8+\delta}$  crystal irradiated along the direction inclined by  $45^\circ$  from the  $c$  axis is in very good agreement with the previous reports on BSCCO irradiated at the same configuration.<sup>53,54</sup>

Our experimental observations are in contradiction with the interpretation of the irreversibility in terms of single pancake depinning from columns, as reported by Van der Beek *et al.*<sup>55</sup> In fact, the directional effect (uniaxial pinning) and critical scaling up the matching field  $B_{\phi}$ , clearly evidenced in our study in Pb-substituted BSCCO, are not in favor that vortices form two-dimensional (2D) Abrikosov pancake vor-

tices pinned by different column sites and the vision that vortex lines are extremely soft. Nevertheless, the experiments done by Van der Beek *et al.* are performed on an optimally doped or a lightly overdoped irradiated BSCCO with the electronic parameter values  $\gamma=360$  and  $550$ , respectively. These values are much higher compared to  $\gamma=60$  measured in our Pb-substituted BSCCO crystals. Numerous studies performed in high- $T_c$  superconductors indicated that the value of the electronic anisotropy strongly affects the static and dynamic properties of the vortex matter in the presence of columnar defects.<sup>2</sup> For example, the 3D Bose-glass was observed at a field below the matching field  $B_\phi$  by the ac magnetic susceptibility measurements in irradiated BSCCO single crystals.<sup>50</sup> Whereas, the Bose-glass behavior was not observed in irradiated  $\text{Bi}_2\text{Sr}_2\text{CuO}_{6+\delta}$  (Bi-2201). This difference is due to the extremely weak coupling between pancake vortices along the  $c$  axis in Bi-2201 ( $\gamma=700$ ) even under the presence of columnar defects.

Finally the main result of this work, which was clearly demonstrated in Fig. 5(a), is that the inclined columnar defects introduced by heavy ion irradiation do not change the vortex dynamics for the solid-to-liquid transition as long as the applied magnetic field is aligned along the CDs. The existence of the Bose-glass behavior indicates that vortex lines are always strongly localized at temperatures below  $T_{\text{BG}}$ . In contrast, when the magnetic field is applied perpendicular to CDs for sample B, there is no way to fit the data to Eq. (1) indicating that the vortex dynamics deviates from the Bose-glass theory. The second observed dip in the  $V(\psi)$  then can only be explained by the pinning efficiency enhancement related to a flux flop phenomenon.

In conclusion, our experimental results show the universality of our observations for both samples. Further investigations are needed in order to understand the behavior in the presence of inclined CDs. The study of the stability of the Bose-glass phase when the applied magnetic field  $\mathbf{H}$  is tilted away from the CDs direction is necessary to clarify the influence of inclined columnar defects on vortex dynamics. The next important point to be explored is to check the existence of a TME in such a configuration of defects.

#### D. Vortex phase diagram

Figure 6 shows a plot of the normalized  $T_{\text{BG}}(\mu_0 H)$  line [i.e.,  $t_{\text{BG}}(f)$ ], extracted from the scaling analysis of each sample. The  $T_{\text{BG}}$  line measured in our previous work<sup>11</sup> of a BSCCO single crystal ( $B_\phi=0.75$  T) irradiated parallel to the  $c$  axis was also shown. As seen from this figure, the Bose-glass lines of all samples have similar features as those reported by Zech *et al.*<sup>18</sup> and Seow *et al.*<sup>53</sup> We observe a pronounced shift of the  $T_{\text{BG}}(B)$  lines for both samples A and B towards higher fields and temperatures due to the presence of CDs. Moreover, the shape of these lines exhibits some features which are not observed in the irreversibility line of the unirradiated reference sample. The first is the presence of a clear kink that occurred in the vicinity of characteristic fields  $B \approx B_\phi$  and  $B \approx B_\phi/3$ , for all samples. We note that the similar form of the Bose-glass line for sample B compared to what is observed for samples irradiated along the  $c$  axis sug-

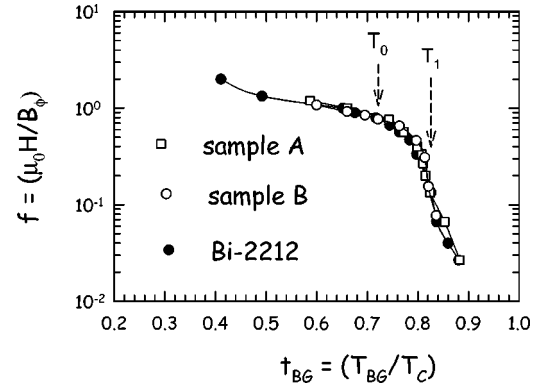


FIG. 6. Semilogarithmic plots of Bose-glass melting line, extracted from scaling analysis. The lines are normalized by the matching field vs normalized temperature dependence for samples A and B over a wide range of filling fractions  $f$ . The  $T_{\text{BG}}(\mu_0 H)$  lines of a BSCCO ( $B_\phi=0.75$  T) irradiated parallel to the  $c$  axis are also reported for comparison to Ref. 11. The data obtained above  $f > 0.9$  were determined by using a low ohmic resistivity criterion  $R_{\text{crit}} \sim 1 \mu\Omega$ .

gests the same pinning properties of CDs with changing temperature and/or applied magnetic field for both directions of irradiation. This implies that the inclination of the CDs does not change the pinning properties compared to irradiation oriented parallel to the  $c$  axis. This result has already been observed in investigations of the irreversibility line in BSCCO single crystals irradiated parallel and at an angle of  $45^\circ$  to the  $c$  axis with the same doses which are equivalent to  $B_\phi=0.5$  T when  $\mathbf{H}$  is applied parallel to CDs.<sup>53</sup>

There is a temperature interval between  $0.72$  and  $0.83 T_c$ , where the Bose-glass melting line for all irradiated samples can be scaled on top of each other. This shows that the enhancements of pinning after irradiation are the same at the same reduced temperature and filling factor. It also implies that in this temperature range, the vortex interactions with CDs are not sensitive to the Pb doping level, dose, or inclination of irradiation. In this regime, the Bose-glass melting line follows the accommodation field  $B^*$  which separates the strongly localized regime where the vortices are localized on the CDs from the collective pinning regime due to vortex-vortex interactions. This can be clearly seen in Fig. 2(b) of Ref. 54, in accordance with Nelson and Vinokur's theory.<sup>5</sup> In fact,  $B^* \approx (C_0/2\xi_{ab})^2 [1 - (T/T_c)]$  decreases linearly above the temperature  $T_0$  up to the depinning temperature  $T_1$ . Beyond this interval, the vortex system is increasingly dominated by vortex-vortex interactions (high field) or thermal fluctuations and/or vortex-vortex interactions (high temperature) in agreement with previous studies on BSCCO single crystals with columnar defects.<sup>38,56,57</sup>

The kinks observed around  $B_\phi/3$  ( $t_{\text{BG}} \sim 0.83$ ) and  $0.8B_\phi$  ( $t_{\text{BG}} \sim 0.72$ ) in the Bose-glass transition lines can be related to the two characteristic temperatures  $T_1$  and  $T_0$  of Refs. 4 and 5, respectively. Indeed, the first temperature  $T_{\text{BG}} \sim 0.72 T_c$  is identified with the crossover temperature  $T_0$  separating the low- and high-temperature limits defined by the relation  $C_0 = 2^{1/2} \xi_{ab}(T_0)$ . Using  $\xi_{ab} = 20 \text{ \AA}$  and  $C_0 = 45 \text{ \AA}$ , we find  $T_0 = [1 - 2(\xi_{ab}/C_0)^2] T_c \sim 0.68 T_c$ . The second tem-

perature  $T_{BG} \sim 0.83T_c$  is related to the depinning temperature  $T_1$ , i.e., the temperature at which the thermal energy becomes comparable to the pinning energy. For the strongly anisotropic BSCCO, the 2D depinning temperature was estimated to be  $T_1 \sim d\alpha\varepsilon_0$ , where  $d$  is the Cu layer spacing,  $\alpha < 1$  is the pinning efficiency of columnar defects, and  $\varepsilon_0 = (\phi^2/4\pi\mu_0\lambda^2)$  is the line tension. Using a typical value of  $d=15 \text{ \AA}$  and our experimental value  $T=0.83T_c$ , one can obtain  $\alpha \sim 0.7$ , which is consistent with other experimental results.<sup>54</sup>

#### IV. SUMMARY

The angular dependence of the current-voltage characteristics over a wide range of filling fraction  $f$  and temperature are used to investigate the vortex dynamics in  $\text{Bi}_{1.8}\text{Pb}_{0.2}\text{Sr}_2\text{CaCu}_2\text{O}_{8+\delta}$  single crystals irradiated by high-energy heavy-ions along the direction inclined by  $\theta_{\text{irr}}=45^\circ$  from the  $c$  axis. This configuration was compared to a crystal irradiated along the  $c$  axis. Above 40 K, angular measurements for both samples reveal that the dissipation in the vortex solid state exhibits the usual anisotropic pinning effect when the vortex lines and CDs are aligned. In both cases, in

this range of temperature, the  $I$ - $V$  characteristics can be described by the scaling laws which were predicted for Bose-glass melting with the same critical exponents. This result implies the existence of the Bose-glass-to-liquid transition at  $T_{BG}(B)$  for magnetic fields ( $f < 1$ ), even for inclined columnar defects. Moreover, for inclined CDs, an additional clear dip was observed when the magnetic field direction is  $-45^\circ$ . Finally, the  $V(\psi)$  curves measured at low temperatures ( $T=20 \text{ K}$ ) reveal two main features in the case of inclined parallel columnar defects: the optimum pinning is obtained for fields applied around the  $c$ -axis direction and the persistence of the directional pinning. It should be noted that the accommodation of the vortices to the tracks was sharply decreased below  $T \sim 40 \text{ K}$ . The dip shift observed at low temperature from the inclined CDs direction toward the  $c$  axis with decreasing  $T$  can be ascribed to a partially pinned staircases vortex structure.

#### ACKNOWLEDGMENTS

We gratefully acknowledge helpful discussions with L. M. Paulius. The authors thank Christophe Honstetter and Micheline Barbey for technical support. This work was supported by the CNRT-Région Centre (France).

\*Corresponding authors. Email address: ammor@delphi.phys.univ-tours.fr

- <sup>1</sup>A. Tonomura, H. Kasai, O. Kaminura, T. Matsuda, K. Harada, Y. Nakayama, J. Shimoyama, K. Kishio, T. Hanaguri, K. Kitazawa, and S. Okayasu, *Nature (London)* **412**, 620 (2001).
- <sup>2</sup>V. Hardy, A. Wahl, S. Hebert, A. Ruyter, J. Provot, D. Groult, and Ch. Simon, *Phys. Rev. B* **54**, 656 (1996).
- <sup>3</sup>T. Schuster, H. Kuhn, M. Indenbom, M. Leghissa, M. Kraus, and M. Konczykowski, *Phys. Rev. B* **51**, 16 358 (1995).
- <sup>4</sup>For a review, see G. Blatter, V. B. Geshkebein, V. B. Larkin, and V. M. Vinokur, *Rev. Mod. Phys.* **66**, 1125 (1994).
- <sup>5</sup>D. R. Nelson and V. M. Vinokur, *Phys. Rev. B* **48**, 13 060 (1993).
- <sup>6</sup>R. C. Budhani, W. L. Holstein, and M. Suenaga, *Phys. Rev. Lett.* **72**, 566 (1994).
- <sup>7</sup>C. J. Van der Beek, M. Konczykowski, V. M. Vinokur, T. W. Li, P. H. Kes, and G. W. Crabtree, *Phys. Rev. Lett.* **74**, 1214 (1995).
- <sup>8</sup>W. Jiang, N. C. Yeh, D. S. Reed, U. Kriplani, D. A. Beam, M. Konczykowski, T. A. Tombrello, and F. Holtzberg, *Phys. Rev. Lett.* **72**, 550 (1994).
- <sup>9</sup>R. J. Olsson, W. K. Kwok, L. M. Paulius, A. M. Petrean, D. J. Hofman, and G. Crabtree, *Phys. Rev. B* **65**, 104520 (2002).
- <sup>10</sup>A. Mazilu, H. Safar, M. P. Maley, J. Y. Coulter, L. N. Bulaevskii, and S. Foltyn, *Phys. Rev. B* **58**, R8909 (1998).
- <sup>11</sup>J. C. Soret, V. Ta Phuoc, L. Ammor, A. Ruyter, R. De Sousa, E. Olive, G. Villard, A. Wahl, and Ch. Simon, *Phys. Rev. B* **61**, 9800 (2000).
- <sup>12</sup>R. Sugano, T. Onogi, K. Hirata, and M. Tachiki, *Phys. Rev. B* **60**, 9734 (1999).
- <sup>13</sup>V. T. Phuoc, E. Olive, R. De Sousa, A. Ruyter, L. Ammor, and J. C. Soret, *Phys. Rev. Lett.* **88**, 187002 (2002).
- <sup>14</sup>J. R. Thompson, Y. R. Sun, H. R. Kerchner, D. K. Christen, B. C.

- Sales, A. D. Marwick, L. Civale, and J. O. Thomson, *Appl. Phys. Lett.* **60**, 2306 (1992).
- <sup>15</sup>L. Klein, E. R. Yacoby, Y. Yeshurun, M. Konczykowski, F. Holtzberg, and K. Kishio, *Physica C* **209**, 251 (1993); *Phys. Rev. B* **48**, 3523 (1993).
- <sup>16</sup>S. Hébert, G. Perkins, M. Abd el-Salam, and A. D. Caplin, *Phys. Rev. B* **62**, 15 230 (2000).
- <sup>17</sup>Y. Kazumata, S. Okayasu, M. Sataka, and H. Kumakura, *Phys. Rev. B* **58**, 5839 (1998).
- <sup>18</sup>D. Zech, S. L. Lee, H. Keller, G. Blatter, B. Janossy, P. H. Kes, T. W. Li, and A. A. Menovsky, *Phys. Rev. B* **52**, 6913 (1995).
- <sup>19</sup>G. Villard, D. Pelloquin, and A. Maignan, *Phys. Rev. B* **58**, 15 231 (1998).
- <sup>20</sup>A. Wahl, D. Thopart, G. Villard, A. Maignan, Ch. Simon, J. C. Soret, L. Ammor, and A. Ruyter, *Phys. Rev. B* **60**, 12 495 (1999).
- <sup>21</sup>A. Ruyter, Ch. Simon, V. Hardy, M. Hervieu, and A. Maignan, *Physica C* **225**, 235 (1994).
- <sup>22</sup>J. Shimoyama, Y. Nakayama, K. Kitazawa, K. Kishio, Z. Hiroi, I. Chong, and M. Takano, *Physica C* **281**, 69 (1997).
- <sup>23</sup>I. Chong, Z. Hiroi, M. Izumi, J. Shimoyama, Y. Nakayama, and M. Takano, *Science* **276**, 770 (1997).
- <sup>24</sup>N. Musolino, S. Bals, G. van Tendeloo, N. Clayton, E. Walker, and R. Flükiger, *Physica C* **401**, 270 (2004).
- <sup>25</sup>L. S. Uspenskaya, A. B. Kulakov, and A. L. Rakhmanov, *Phys. Rev. B* **68**, 104506 (2003); *Physica C* **402**, 136 (2004).
- <sup>26</sup>S. Herbert, V. Hardy, G. Villard, M. Hervieu, Ch. Simon, and J. Provost, *Phys. Rev. B* **57**, 649 (1998).
- <sup>27</sup>H. Raffy, S. Labdi, O. Laborde, and P. Monceau, *Phys. Rev. Lett.* **66**, 2515 (1991).
- <sup>28</sup>M. Baziljevich, D. Giller, M. Mcelfresh, Y. Abulafia, Y.



- Radzyner, J. Schneck, T. H. Johansen, and Y. Yeshurun, *Phys. Rev. B* **62**, 4058 (2000).
- <sup>29</sup>A. Pomar, L. Martel, Z. Z. Li, and H. Raffy, *Phys. Rev. B* **63**, 134525 (2001).
- <sup>30</sup>F. Warmont, V. Hardy, Ch. Goupil, Ch. Simon, J. Provot, and A. Ruyter, *Physica C* **277**, 61 (1997).
- <sup>31</sup>K. E. Gray, J. D. Hettinger, D. J. Miller, B. R. Washburn, C. Moreau, and C. Lee, *Phys. Rev. B* **54**, 3622 (1996).
- <sup>32</sup>A. Pomar, L. Martel, Z. Z. Li, O. Laborde, and H. Raffy, *Phys. Rev. B* **63**, 020504(R) (2001).
- <sup>33</sup>B. Holzapfel, G. Kreiselmeyer, S. Bouffard, S. Klaumuzer, and L. Schultz, *Phys. Rev. B* **48**, 600 (1993).
- <sup>34</sup>R. J. Drost, C. J. Van der Beek, J. A. Heijn, M. Konczykowski, and P. H. Kes, *Phys. Rev. B* **58**, R615 (1998).
- <sup>35</sup>F. Hilmer, G. Jacob, P. Haibach, U. Frey, Th. Kluge, H. Adrian, G. Wirth, E. Jager, and E. Schimpf, *Physica C* **311**, 11 (1999).
- <sup>36</sup>R. J. Drost, C. J. Van der Beek, H. W. Zandbergen, M. Konczykowski, A. A. Menovsky, and P. H. Kes, *Phys. Rev. B* **59**, 13 612 (1999).
- <sup>37</sup>S. Hébert, V. Hardy, G. Villard, M. Hervieu, Ch. Simon, and J. Provot, *Physica C* **299**, 259 (1998).
- <sup>38</sup>S. Hébert, V. Hardy, Ch. Simon, and J. Provot, *Phys. Rev. B* **60**, 13 175 (1999).
- <sup>39</sup>A. Tonomura, H. Kasai, O. Kaminura, T. Matsuda, K. Harada, Y. Nakayama, J. Shimoyama, K. Kishio, T. Hanaguri, K. Kitazawa, and S. Okayasu, *Physica C* **369**, 68 (2002).
- <sup>40</sup>J. C. Soret, L. Ammor, B. Martinie, Ch. Goupil, V. Hardy, J. Provot, A. Ruyter, and Ch. Simon, *Physica C* **220**, 242 (1994).
- <sup>41</sup>A. V. Silhanek, L. Civale, and M. A. Avila, *Phys. Rev. B* **65**, 174525 (2002); A. V. Silhanek, L. Civale, S. Candia, and G. Nieva, *ibid.* **59**, 13 620 (1999); M. A. Avila, L. Civale, A. V. Silhanek, R. A. Ribeiro, O. F. de Lima, and H. Lanza, *ibid.* **64**, 144502 (2001).
- <sup>42</sup>K. Itaka, H. Taoka, S. Ooi, T. Shibauchi, and T. Tamegai, *Phys. Rev. B* **60**, R9951 (1999).
- <sup>43</sup>M. Dhallé, C. Beneduce, N. Musolino, R. Gladyshevskii, E. Walker, and R. Flukiger, *IEEE Trans. Appl. Supercond.* **11**, 3646 (2001).
- <sup>44</sup>N. Musolino, S. Bals, G. Van Tendeloo, N. Clayton, E. Walker, and R. Flükiger, *Physica C* **399**, 1 (2003).
- <sup>45</sup>W. K. Kwok, L. M. Paulius, V. M. Vinokur, A. M. Petrean, R. M. Ronningen, and W. Crabtree, *Phys. Rev. Lett.* **80**, 600 (1998).
- <sup>46</sup>T. Sueyoshi, N. Ishikawa, A. Iwase, Y. Chimi, T. Kiss, T. Fujiyoshi, and K. Miyahara, *Physica C* **309**, 79 (1998).
- <sup>47</sup>R. Prozorov, M. Konczykowski, B. Schmidt, Y. Yeshurun, A. Shaulov, C. Villard, and G. Koren, *Phys. Rev. B* **54**, 15 530 (1996).
- <sup>48</sup>C. Reichhardt, A. van Otterlo, and G. T. Zimanyi, *Phys. Rev. B* **84**, 1994 (2000).
- <sup>49</sup>A. Vestergren, J. Lidmar, and M. Wallin, *Phys. Rev. B* **67**, 092501 (2003); J. Lidmar and M. Wallin, *Europhys. Lett.* **47**, 494 (1999); M. Wallin, E. S. Sorensen, S. M. Girvin, and A. P. Young, *Phys. Rev. B* **49**, 12 115 (1994).
- <sup>50</sup>N. Kuroda, N. Ishikawa, Y. Chimi, A. Iwase, R. Yoshzaki, and T. Kambara, *Physica C* **321**, 143 (1999).
- <sup>51</sup>V. Ta Phuoc, A. Ruyter, L. Ammor, A. Wahl, and J. C. Soret, *Phys. Rev. B* **56**, 122 (1997).
- <sup>52</sup>G. L. Bhalla and U. Divakar, *Physica C* **355**, 103 (2001).
- <sup>53</sup>W. S. Seow, R. A. Doyle, A. M. Campbell, G. Balakrishnan, D. Mck. Paul, K. Kadowaki, and G. Wirth, *Phys. Rev. B* **53**, 14 611 (1996).
- <sup>54</sup>D. Zech, S. L. Lee, H. Keller, G. Blatter, P. H. Kes, and T. W. Li, *Phys. Rev. B* **54**, 6129 (1996).
- <sup>55</sup>C. J. van der Beek, M. Konczykowski, A. V. Samoilov, N. Chikumoto, S. Bouffard, and M. V. Feigel'man, *Phys. Rev. Lett.* **86**, 5136 (2001).
- <sup>56</sup>M. O. Mun, S. I. Lee, P. C. Cranfield, B. K. Cho, and D. C. Johnston, *Phys. Rev. Lett.* **76**, 2790 (1996).
- <sup>57</sup>B. Khakovich, E. Zeldov, D. Majer, T. W. Li, P. H. Kes, and M. Konczykowski, *Phys. Rev. Lett.* **76**, 2555 (1996).